

Effect of reclaimed sand additions on mechanical properties and fracture behavior of furan no-bake resin sand

Yan-lei Li¹, *Guo-hua Wu¹, Wen-cai Liu¹, An-tao Chen¹, Liang Zhang¹, and Ying-xin Wang^{1,2}

1. National Engineering Research Center of Light Alloy Net Forming and State Key Laboratory of Metal Matrix Composites, School of Materials Science and Engineering, Shanghai Jiao Tong University, Shanghai 200240, China;

2. Shanghai Light Alloy Net Forming National Engineering Research Center Co., Ltd., Shanghai 201615, China

Abstract: In this work, the effects of reclaimed sand additions on the microstructure characteristics, mechanical properties and fracture behavior of furan no-bake resin sand have been investigated systematically within the temperature range from 25 to 600 °C. The addition of 20%–100% reclaimed sand showed dramatic strength deterioration effect at the same temperature, which is associated with the formation of bonding bridges. Both the ultimate tensile strength (UTS) and compressive strength (CS) of the moulding sand initially increase with the increase of temperature, and then sharply decrease with the further increase of temperature, which is attributed to the thermal decomposition of furan resin. The addition amount of reclaimed sand has a remarkable effect on the room temperature fracture mode, i.e., with the addition of 0–20% reclaimed sand, the fracture mode was mainly cohesive fracture; the fracture mode converts to be mixture fracture mode as the addition of reclaimed sand increases to 35%–70%; further increasing the addition to 100% results in the fracture mode of typical adhesive fracture. The fracture surface of the bonding bridge changes from a semblance of cotton or holes to smooth with the increase of test temperature.

Key words: reclaimed sand; mechanical properties; thermal decomposition; fracture mode

CLC numbers: TG221+.2

Document code: A

Article ID: 1672-6421(2017)02-128-10

Furan no-bake resin sands possess a good combination of high dimension accuracy, good surface finish, and room temperature curing, which make them attractive for industrial applications of producing moulds for different kinds of castings, such as steel, iron and non-ferrous alloy castings [1–3]. However, it is commonly considered that after pouring, the furan no-bake resin sand may exhibit some shortcomings, such as poor collapsibility, various types of gases released, residual resin, and waste sand, which would cause environmental pollution, increased casting production cost and waste of natural resources [4,5]. Furthermore, the foundry industry is under great pressure due to national policy restrictions on resource conservation and environmental protection [6–9]. Therefore, the low cost, effective, and eco-friendly furan

resin sands are still under investigation.

The application of reclaimed sand has a clear economical advantage for mass production of components due to their short reprocessing cycle and low assembly costs. Previous research found the possibility of reclaimed sand in casting, i.e., green moulding sand [10–15], furan resin sand [16–19], and sodium silicate sand [20–22]. It was found that the mixture of reclaimed sand and new sand satisfies the standards for moulding sands, and sustainable sand casting was developed. In the process of casting, heat will be generated through liquid metals so that the temperature of the moulding sand may be quite high. Thus, the high temperature property is one of the main parameters of moulding sand. In order to meet the requirements of a realistic application environment which requires long-life service at high temperature, excellent mechanical performance at elevated temperature is a primary demand for moulding sands. In addition, the influence of reclaimed sand content on the mechanical properties of moulding sand at elevated temperatures is still to be clarified. Therefore, a good understanding of the relationship between the reclaimed sand content and the

*Guo-hua Wu

Male, born in 1962, Professor, Ph.D. He focuses his research on advanced Mg/Al alloys and their precise forming technologies. To date, he has published over 160 papers and obtained 61 Chinese patents.

E-mail: ghwu@sjtu.edu.cn

Received: 2016-03-01; Accepted: 2016-11-20

mechanical properties at elevated temperature is needed.

In this study, the effects of reclaimed sand content on the mechanical properties and fracture modes of furan no-bake resin sand were investigated. The relationship between mechanical properties and fracture mode was discussed, and the mechanism for the variation of mechanical properties at temperatures ranging from 25 to 600 °C was revealed. The present study would provide the foundation for the development of furan no-bake resin sand.

1 Experimental procedures

1.1 Raw materials

Four types of raw materials were used in this study: new sand, reclaimed sand, furan resin binder, and catalyst. According to the national standards of the People's Republic of China (GB/T2684-2009)^[23], the properties including water content, clay content, loss on ignition (LOI), particle size and pH value of new sand and reclaimed sand are given in Table 1.

Table 1: Characteristics of new sand and reclaimed sand

Sand	Water content (wt.%)	Clay content (wt.%)	LOI (%)	Particle size distribution (mesh)	pH value
New sand	0.35	0.025	0.8	50/100	9.16
Reclaimed sand	0.83	0.33	2.15	50/100	5.17

The new sand was Dalin scrubbed sand (50/100 meshes) with a sediment percentage of less than 0.2%. The reclaimed sand (50/100 meshes) was obtained from a casting factory in China. The reclaimed sand was fabricated by dry mechanical process with a sediment percentage of less than 0.5%. The furan resin binder (viscosity is 99.5 mPa·s, and free formaldehyde is 0.21%) and the catalyst (total acid is 24.89%, and the free acid is 7.94%) were from Xingye, Suzhou, China.

1.2 Mix design

The reclaimed sand was mixed with the new sand with ratios of 0% (new sand), 20%, 35%, 50%, 70% and 100% (all addition percentages are in weight throughout this article unless noted), respectively. For all mixtures, the amount of the furan resin binder was 1.2%. The dosage of catalyst was kept at 40% of total furan resin binder.

1.3 Samples preparation

The new sand and reclaimed sand were mechanically mixed in an automatic sand mixer for 1 min, then the catalyst was added and mixed with the sand for 2 min. After that, the furan resin binder was added into the mixture and stirred for 1 min. Finally, the mixture was poured into a permanent mold compacted by vibrating table, and held for 24 hours until complete hardening.

1.4 Analysis methods

Water content testing was carried out on SGH infrared drying apparatus. The water content was calculated as follows: $W = [(M2 - M1) / M2] \times 100\%$, where W is the water content, $M1$ is the weight of the silica sand samples treated with drier, and $M2$ is the weight of the silica sand samples untreated with drier. Clay content testing was carried out on SXW vortex type washing sand washer. The clay content was calculated as follows: $C = [(C2 - C1) / C2] \times 100\%$, where C is the clay content, $C2$ is the weight of the silica sand samples untreated with washer, and $C1$ is the weight of the silica sand samples treated with washer. Powder content testing was carried out on SSZ sand screener, and the silica sand was shaken vigorously. The silica sand

particles passing through a 140 mesh sieve are identified as powder in this work. Acid demand value (ADC) testing was performed on a magnetic stirrer. About 50 ± 0.1 g silica sand samples were immersed into a beaker containing 50 mL of distilled water, and then 50 mL of $0.1 \text{ mol} \cdot \text{L}^{-1}$ HCl solution was also added. The mixture was stirred for 5 min by magnetic stirrer. After 1 hour stewing, $0.1 \text{ mol} \cdot \text{L}^{-1}$ HCl was gradually neutralized by $0.1 \text{ mol} \cdot \text{L}^{-1}$ NaOH solution, and the optimum pH of the neutralized solution was in the range of 3.0 to 5.0. ADC value is calculated from the equation: $A = A1 - A2$, where A is the acid demand value, $A1$ is the consumption of $0.1 \text{ mol} \cdot \text{L}^{-1}$ NaOH solution (mL) by a blank test, and $A2$ is the consumption of $0.1 \text{ mol} \cdot \text{L}^{-1}$ NaOH solution (mL) by silica sand samples.

Tensile testing was carried out on a XYQ-II uniaxial material test machine at a crosshead speed of $1 \text{ mm} \cdot \text{min}^{-1}$ at room temperature. The dimensions of these specimens are given in Fig. 1(a). Compressive strength (CS) testing was carried out on a SQW-A high temperature strength testing machine equipped with a heating chamber at the initial strain rate of $1 \text{ mm} \cdot \text{min}^{-1}$. The cylindrical samples for compression testing have a dimension of 50 mm in gauge length and 25 mm in diameter as shown in Fig. 1(b). For tests at elevated temperatures, specimens were heated to the required temperature prior to testing. Temperatures of specimens were measured using a K-type thermocouple located at the central portion of the specimens. The temperatures together with the corresponding times were continuously recorded (Fig. 2 and Table 2). When testing the high temperature residual strength, the specimens were heated to the required temperature, and then cooled to the room temperature in the air. Under each condition, three specimens were measured and the average value used. Samples and fracture surfaces were analyzed by a scanning electron microscope (SEM, FEI SIRION 200, FEI Company, Hillsboro, Oregon) equipped with an energy dispersive spectroscopy (EDS) detector. Thermo-gravimetric analysis was carried out with a TGAQ600 (TA Instruments, Newcastle, DE, USA). The sample was heated from 25 to 900 °C at $10 \text{ }^\circ\text{C} \cdot \text{min}^{-1}$ under air flow of $100 \text{ mL} \cdot \text{min}^{-1}$.

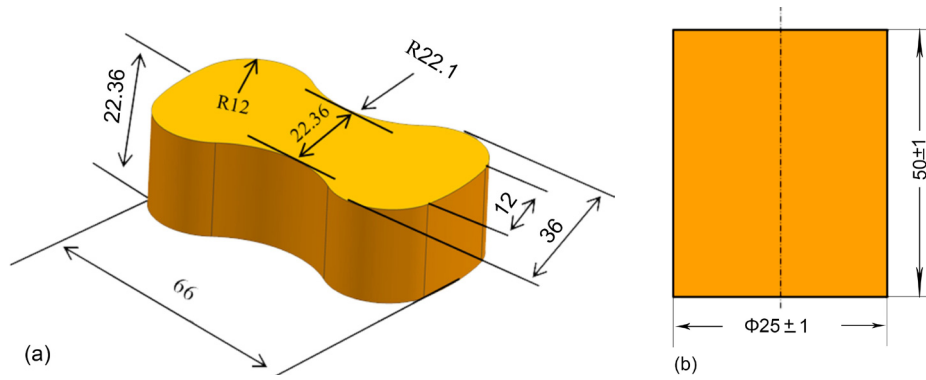


Fig. 1: (a) Dimension (mm) of samples for tensile testing, and (b) dimension (mm) of cylindrical samples for compressive testing

Table 2: Actual preheating temperature and time of samples

Parameters												
T (°C)	100	150	200	250	300	350	400	450	500	550	600	
Time (min)	67	61	45	40	38	32	25	18	14	10.5	5.5	

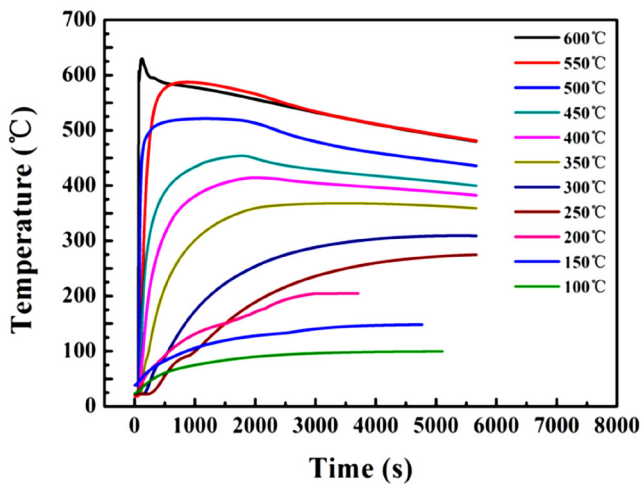


Fig. 2: Preheating temperature curves of the center of tested moulding sand samples

2 Results

2.1 Characteristics of new sand and reclaimed sand

Figures 3 (a) and (b) show the typical SEM images of new sand and reclaimed sand, respectively. Ellipsoid-shape new sand grains are throughout the image mapping, and some spherical sand grains can also be observed [Fig. 3(a)]. The surface of new sand grains is more flat compared to that of the reclaimed sand grains [Fig. 3(b)]. All of sand grains are point-shape particles and with the feature of river patterns. Moreover, lots of point-shape particles can be found on the surface of reclaimed sand grains [Fig. 3(b)], which is due to the dispersing effect caused by impurity particles which mainly consist of powder and clay particles.

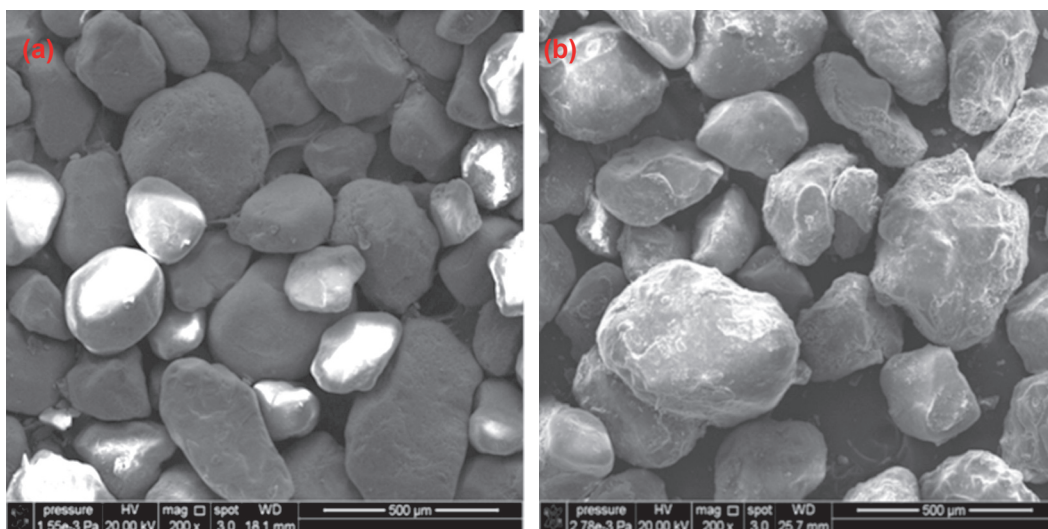


Fig. 3: Typical SEM micrographs of sand grains: (a) new sand and (b) reclaimed sand

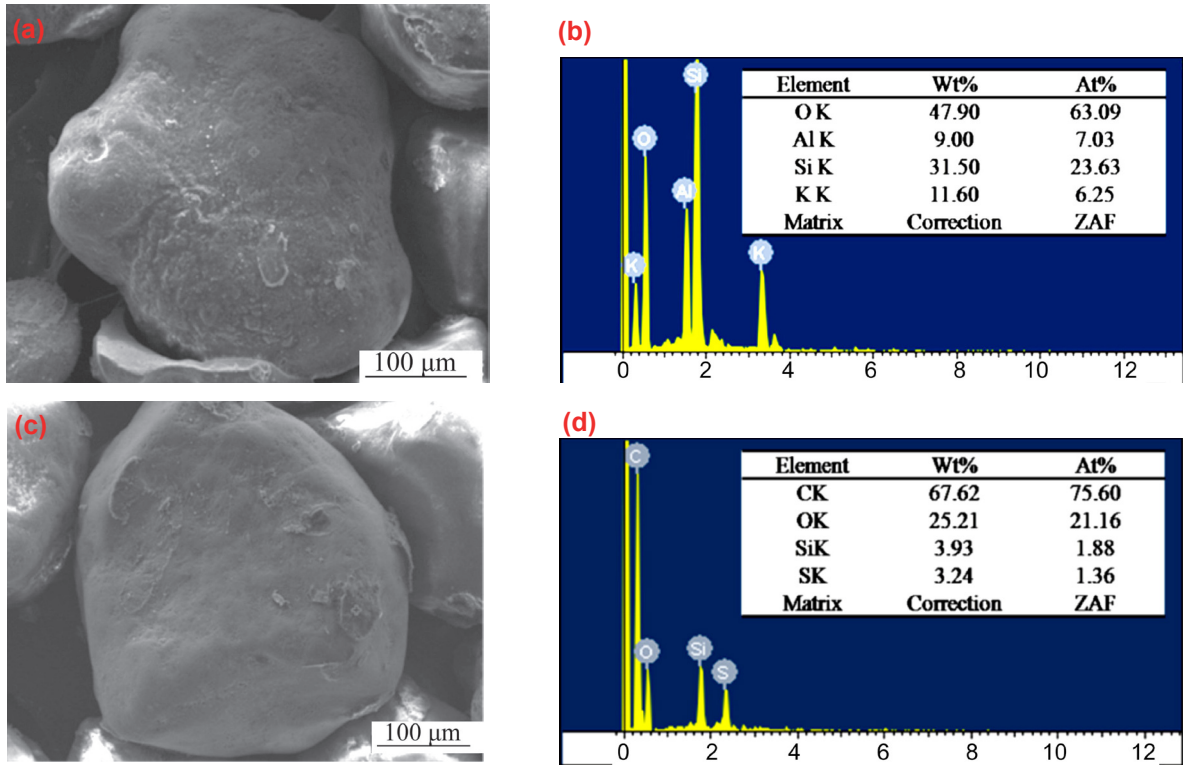


Fig. 4: Typical SEM micrographs and EDS results of different sands: (a) SEM image of new sand, (b) EDS spectrum of new sand grain surface, (c) SEM image of reclaimed sand, and (d) EDS spectrum of reclaimed sand surface

Figure 4 shows the results of EDS analysis of the new sand and reclaimed sand surfaces, respectively. The peak equivalent to aluminum and silicon was detected [Fig. 4(b)]. However, the peak equivalent to sulfur and carbon was detected as shown in Fig. 4(d). This is probably due to the furan resins carbonized by the heat of molten metal, and then deposited on the sand grain surface [16]. It should be pointed out that the reclaimed sand was fabricated by dry methods, and this indicates that the presence and distribution of residual furan resins, curing agent and other impurities were still attached or mixed within sand grains.

Figure 5 shows the weight loss obtained during the heating of the furan resin binder and the corresponding derivative weight loss curve (polymer thermal decomposition is more commonly studied under inert atmospheres, while the oxidative decomposition is equally important because it is closer to the realistic atmospheric conditions of degradation). The first thermal decomposition temperature corresponding to 16% and 5% of weight loss is ~66 °C and ~98 °C, respectively. The former attributes to desorption of the solvent molecules from the resin present in the lattice, while the latter corresponds to dehydration [24]. Between the temperature range from 150 °C to 300 °C, the mass loss is about 35% of the total mass, and the second thermal decomposition stage is probably related to the chain scission of weak chemical bonds [25]. The third decomposition steps appear at the temperature range from 450 °C to 650 °C, and it can be inferred that methylene scission is mainly responsible for the decomposition of furan resin [26, 27].

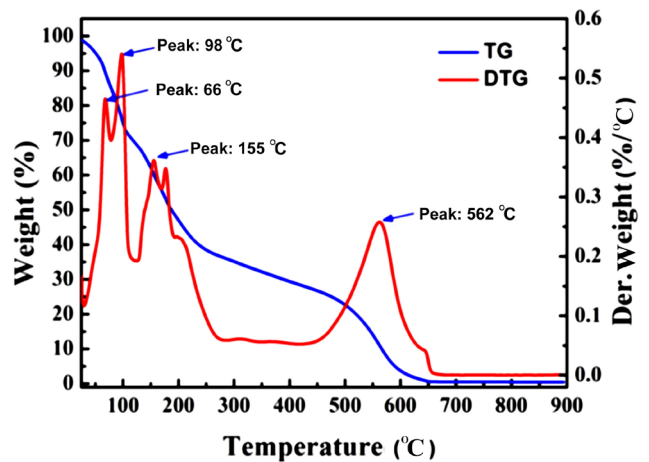


Fig. 5: TG-DTA curves of furan resin

2.2 Effect of reclaimed sand addition on clay content, powder content, water content and acid demand value

In order to have a systematic clarification of the effect of reclaimed sand content (ranging from 0 to 100%) on the moulding sand, the parameters of mixed sand such as clay content, powder content and acid demand value were investigated. Figure 6 shows the parameters of moulding sand with different addition levels of the reclaimed sand. Compared with the new sand, all of the parameters of mixed sand continually increase with the increase of the addition level of reclaimed sand from 20% to 100%.

2.3 Mechanical properties

2.3.1 Room temperature mechanical properties

Figure 7 shows the room temperature tensile strength of the specimens with different additions of reclaimed sand. The tensile strength (TS) was continuously decreased with the increase of additions of reclaimed sand. With the addition of 20% and 35% reclaimed sand, the tensile strength of the sand was decreased from 1.3 MPa to 1.14 MPa and to 1.02 MPa, respectively. When the reclaimed sand content was further increased to 50% and 70%, the tensile strength was remarkably reduced to 0.96 MPa and 0.76 MPa, respectively. As the reclaimed sand content was increased to 100%, the tensile strength decreased to 0.4 MPa.

Figure 8 shows the room temperature compressive strength of the specimens with different additions of reclaimed sand. With increasing reclaimed sand content from 0 to 20% and then to 35%, the compressive strength decreases from 5.2 MPa to 4.6 MPa and then further to 4.5 MPa. When the reclaimed sand content was further increased to 50% and 70%, the compressive strength was reduced to 4.2 and 2.9 MPa, respectively. As the reclaimed sand content was increased to 100%, the compressive strength was remarkably decreased to 1.1 MPa.

2.3.2 Elevated temperature mechanical properties

Figure 9 shows the variation of compressive strength of the moulding sand with different addition levels of reclaimed sand as a function of the temperature. Compared with the room temperature, the moulding sand exhibits higher strength at the temperature range of 100–300 °C. However, as the temperature is above 300 °C, the strength of the moulding sand significantly decreases, and the additions of reclaimed sand have a negligible influence on the strength. In addition, it was worth noting that the compressive strength of the moulding sand initially increases followed by a sharp decrease with the increase of temperature. On the other hand,

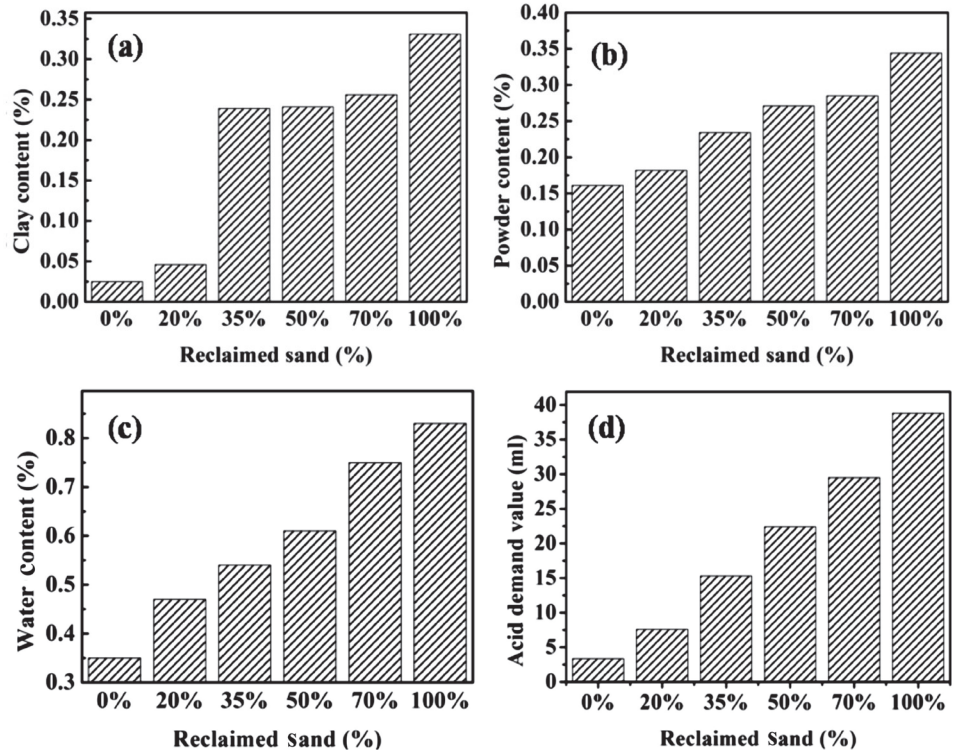


Fig. 6: Parameters of mixture sand under different reclaimed sand additions: (a) clay content, (b) powder content, (c) water content, and (d) acid demand value

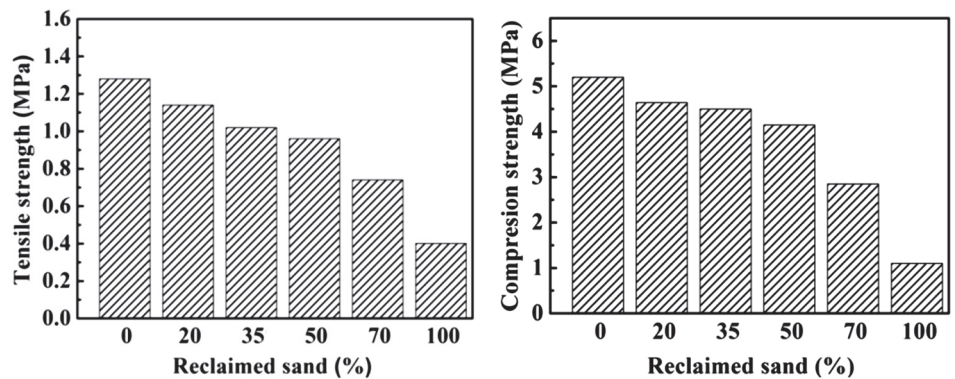


Fig. 7: Tensile properties of tested moulding sand with different reclaimed sand addition levels

Fig. 8: Compressive properties of tested moulding sand with different reclaimed sand addition levels

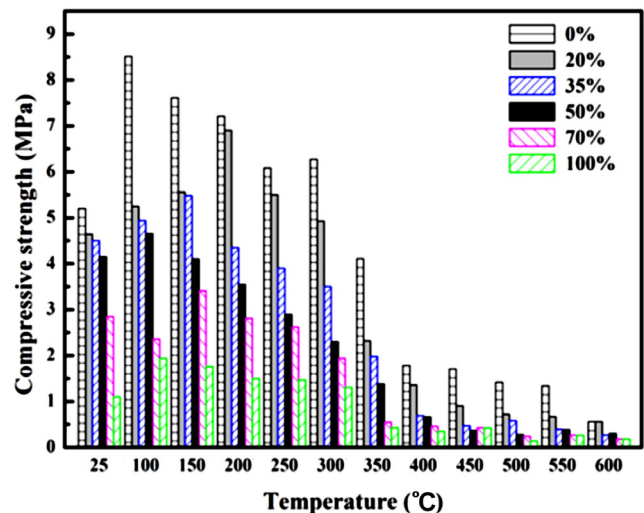


Fig. 9: Compressive strength of moulding sand containing different levels of reclaimed sand

the strength of the specimens remarkably decreases with the increase of content of reclaimed sand at the same temperature. The strength of a mould produced from new sand without the addition of reclaimed sand was higher than that of the counterparts containing 20%–100% reclaimed sand, especially in the temperature range of 25 to 350 °C. However, further increasing the content of reclaimed sand to 100% led to a slight change in compressive strength except in the temperature range of 350–600 °C.

Figure 10 shows the high temperature residual strength of the moulding containing different levels of reclaimed sand. When the temperature for the compression test was 25 °C, the residual strength was continuously decreased with the increase of additions of reclaimed sand. Compared with the room temperature, when the temperature for compression test was between 100 °C and 150 °C, a large improvement of the residual strength was observed, and the peak strength was achieved at 150 °C. However, as the temperature is above 200 °C, the strength of the moulding sand significantly decreases, and the additions of reclaimed sand have a significant influence on the strength. When the temperature was further increased from 300 °C to 400 °C, the residual strength was continuously decreased. In addition, the image mapping results confirmed that the residual strength of moulding containing different levels of reclaimed sand was approximately to 0 MPa in the temperature range of 450–600 °C.

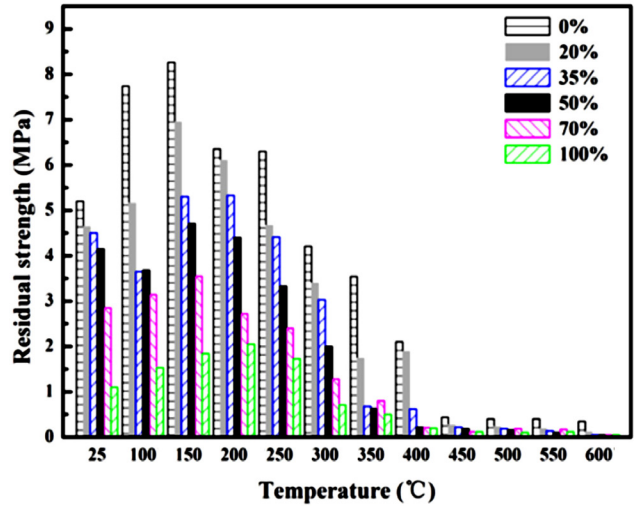


Fig. 10: Residual strength of moulding sand containing different levels of reclaimed sand

2.4 Fracture behavior

Figure 11 shows the images of typical fracture surfaces of tensile specimens with different addition levels of reclaimed sand at room temperature. All of the failure surfaces consist of fractured bonding bridges and sand grains (marked by arrows). When the content of reclaimed sand was 0 and 20%, the fracture surface presented many ruptured bonding bridges

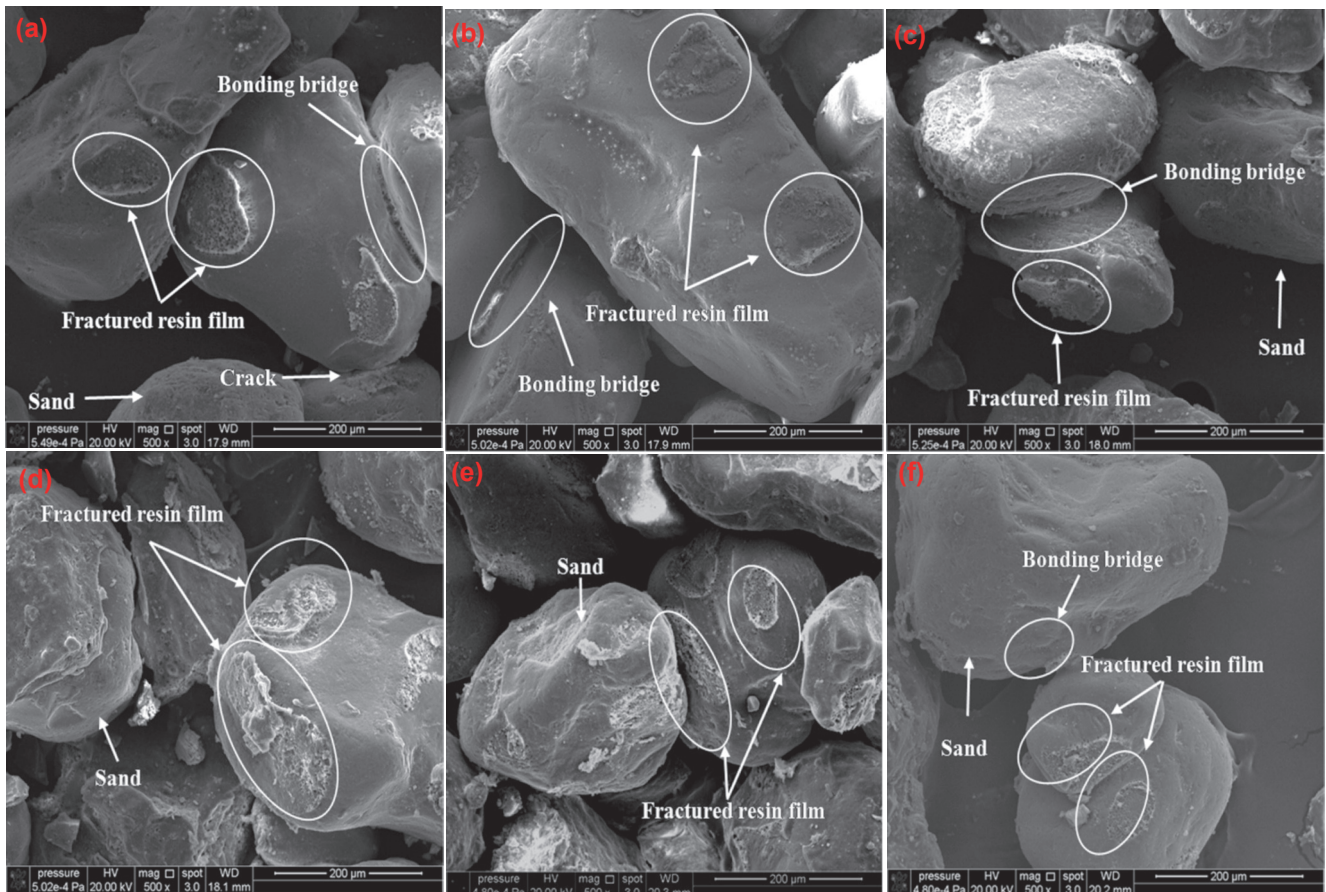


Fig. 11: Typical SEM micrographs of tensile fracture surfaces of specimens with different reclaimed sand contents: (a) 0, (b) 20%, (c) 35%, (d) 50%, (e) 70%, and (f) 100%

with micro-cracks. The morphology of the broken bonding bridge has the semblance of cotton and holes, indicating that after the micro-cracks form inside the bonding bridge, they propagate along the bridge interface by connecting with others or across the bonding bridge as cohesive fracture. When the addition level of reclaimed sand was increased to 35%–70%, the fracture surfaces show many flat and dented areas on the grain surface [Fig. 11(c–e)], cracks, and even small holes are observed on the fracture surface. The cracks are mostly formed on bonding bridge or grain surface, indicating the fracture mode of specimens is mixed fracture (cohesive and adhesive fracture). These results are consistent with Ref. [28]. As 100% reclaimed sand was added, the fracture surface of the resin film becomes dented [Fig. 11(f)], the micro-cracks nucleate at the interface of the resin film and grain surface, propagate along the sand grain surface, and finally lead to the peeling off resin film on the sand grains. In this condition, the fracture surface of the specimens is dominated by adhesive fracture.

Figure 12 shows the typical fracture surface images of compressive specimens with different addition levels of reclaimed sand at room temperature. It can be observed that the fracture surfaces consist of some broken bonding bridges and sand grains [Fig. 12(a)]. A few dimples and micropores were also observed. Therefore, the fracture mode of the compressive specimens is cohesive fracture. By increasing the reclaimed

sand content to 70%, both of fractured bonding bridge and peeling off of resin film were easily found at the fracture surface [Fig. 12(b)–(c)], suggesting that the fracture mode of specimens gradually changes from cohesive fracture to mixed fracture. When the reclaimed sand content was 100%, the morphology of the fracture surface was similar with Fig. 11(d), i.e. shows obvious adhesive fracture.

Figure 13 shows typical SEM images of fracture surfaces of the new sand specimens under different temperatures (in order to avoid the influence of impurities of reclaimed sand on the fracture surface, the moulding sand without reclaimed sand addition was found to be the optimal choice for SEM examination). When the specimen was tested at 100 °C, it could be seen that the fracture surface showed large sand grains, bonding bridge and fractured resin film [Fig. 13(a)], and the fracture mode tested at 100 °C was cohesive fracture. When the specimen was tested at 250 °C, the fracture surface consisted of ruptured bonding bridge and grain sand, which indicated a cohesive fracture. However, in the fracture surface of specimens tested at 450 °C, it was seen that the fractured resin film surface was much more flat compared with the specimens tested at 100 °C and 250 °C. In addition, lots of fractured flat resin film surfaces can be found at 600 °C [Fig. 13(d)], which is mainly due to the thermal decomposition of resin film.

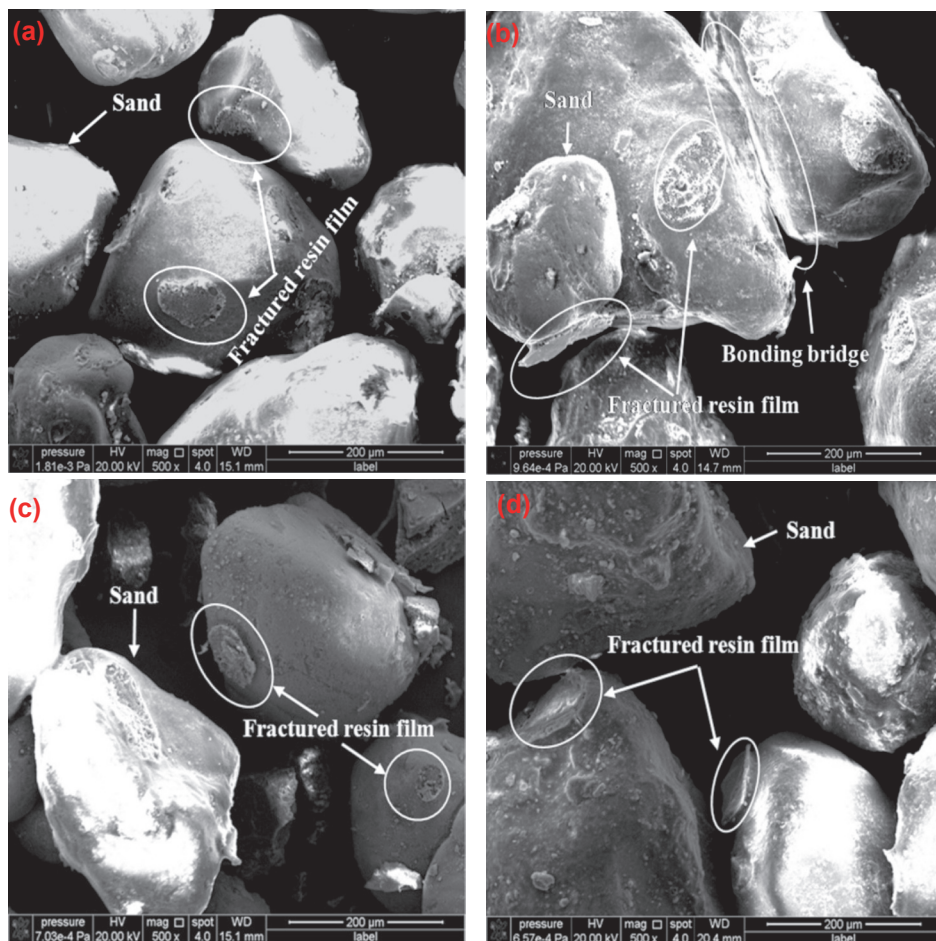


Fig. 12: Typical SEM images of compressive fracture surfaces of specimens with different reclaimed sand contents: (a) 0, (b) 35%, (c) 70%, and (d) 100%

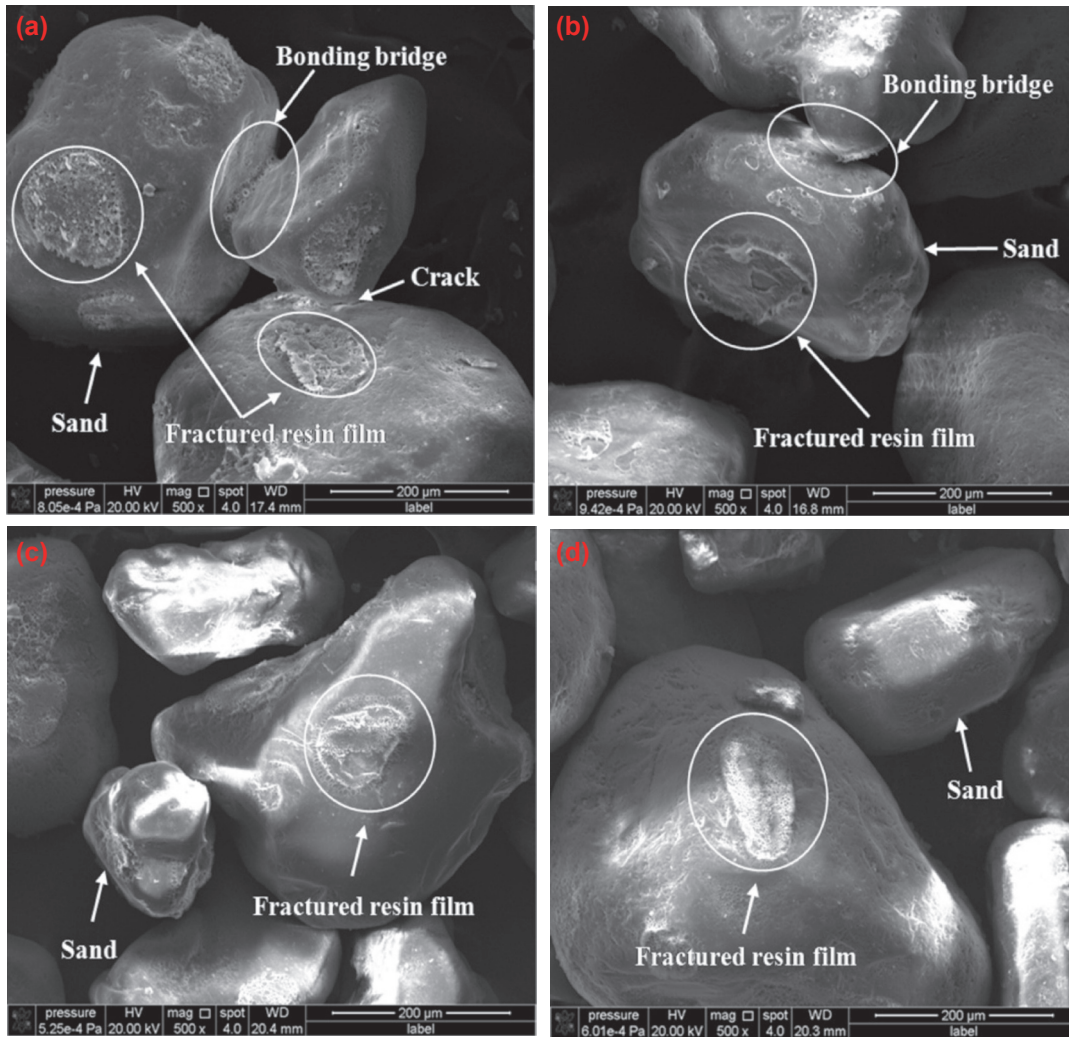


Fig. 13: Typical SEM images of compressive fracture surfaces of specimens at elevated temperatures: (a) 100 °C, (b) 250 °C, (c) 450 °C, and (d) 600 °C

3 Discussion

In this study, the addition of reclaimed sand to produce furan no-bake resin mouldings brings a dramatic decrease in mechanical properties at each temperature. This phenomenon is explained in the following paragraphs.

Increasing the addition level of reclaimed sand significantly deteriorates the mechanical properties of the sand moulding. The decrease of the mechanical properties of the sand moulding was attributed to the increase of powder content, acid demand value and mud content [29]. Furthermore, the SEM micrograph of the reclaimed sand confirmed that a large number of residual binders were coated on the surface of the reclaimed sand (Figs. 3 and 4). It has been reported that the residual binder attached on the reclaimed sand can increase the acid demand value of the reclaimed sand [18]. Moreover, the result of EDS analysis of the reclaimed sand indicates that the residual curing agent exists on the surface of grain, which would increase the consumption of furan resin binder. Furthermore, the presence of an amount of mud or powder also consumed furan resin binder, which would lead to the decrease of the strength [17]. Ding and Kayal also found that water always existed in the resin film, which caused the formation of small holes within the cold-setting resin binder

and consequently reduced cohesive strength [1, 29]. Therefore, the addition of the reclaimed sand can increase the acid demand value and furan resin binder.

The mechanical property of the sand moulding is closely related to the bonding bridge of moulding sand. Although the main impurities (powder, clay and residual resin binder) have an adverse effect on the mechanical properties of the moulding, the influence is limited due to the content of impurities. Figures 11 and 12 show the SEM images of fracture surfaces of the sand moulding specimens with different contents of the reclaimed sand. With the addition of 0–20% reclaimed sand, the fracture mode was mainly cohesive fracture; the fracture mode converts to be mixture fracture mode as the addition of reclaimed sand increases to 35%–70%; further increasing the addition to 100%, the fracture mode is typical adhesive fracture. This is considered to be associated with the resin film coated on the grain surface after the addition of reclaimed sand, which would result in the decrease of adhesive strength [30]. When the temperature increases from 100 to 250 °C, the fracture mode remains identical [Fig. 13(a) and (b)]. However, as the temperature further increases to 450 °C the fracture surface of bonding bridge is much more smooth than that at 100 °C and 250 °C

[Fig. 13(d)]. The deterioration in the mechanical properties of sand moulding is associated with the self-collapsibility of sand grains, which is due to the decomposition of the bonding bridge at elevated temperatures, particularly at 450 °C and above (Fig. 4). The large decrease of strength was also attributed to thermal decomposition of cured furan resin.

Both residual strength and compressive strength of the sand moulding initially increase with the increase of temperature and then decrease as the temperature further increases. According to the TG-DTA results, the first mass loss between room temperature and 150 °C corresponds to the vaporization of solvent moisture and desorption of water which might be the main reason for the increase of the strength of the sand moulding within the temperature range of 25 to 150 °C. Similar results have been observed in previous reports on clay^[31,32] and sodium silicate^[33] moulding sands. When the preheating temperature was increased to 150–400 °C, the thermal decomposition of resin film is probably related to the chain scission of weak chemical bonds. An important feature of this stage is that the fractured resin films show a smooth surface [Fig. 13(b-c)], which further confirms that fractured resin films are not thermally stable enough to resist compression at elevated temperatures. When the temperature was further increased from 400 °C to 650 °C, the thermal decomposition of resin films prevents cohesiveness of the sand grains. Finally, an overall decrease in strength of the specimen can be observed with the increase of the test temperature. The addition of the reclaimed sand leads to decrease of the strength of specimens at each temperature. This is also considered to be associated with the decomposition of the resin film after the preheating treatment, which results in the fracture of the bonding bridge and consequently weaker compressive strength after the testing. Suitable preheating temperature for specimens can lead to improvement in the strength of the specimen, while high temperatures tend to cause the thermal decomposition of resin film, and cracks are initiated and accelerate the failure of specimens.

4 Conclusions

In this study, the influence of the addition level of reclaimed sand on microstructure, high-temperatures mechanical behaviors, and fracture modes of no-bake furan resin sand were investigated systematically. The main conclusions can be summarized as follows:

(1) Increasing the addition level of reclaimed sand significantly deteriorates the mechanical properties of the sand moulding at each temperature. The addition of 70% and 100% reclaimed sand exhibited relatively low tensile strength and compressive strength at both room and elevated temperatures.

(2) The sand moulding exhibits significant anomalous strength behavior in the temperature range of 25 to 600 °C. Both residual strength and compressive strength of the sand moulding initially increase with the increase of test temperature, and then decrease as the test temperature increases further.

(3) With additions of 0–20% reclaimed sand, the fracture

mode of mouldings is mainly cohesive. As the addition of reclaimed sand increases to 35%–70%, the fracture mode converts to mixed fracture. Typical adhesive fracture was observed when the content of reclaimed sand increases to 100%. The additions of 20%–50% reclaimed sand to moulding sand show a moderate strength at room and elevated temperatures.

References

- [1] Ding G L, Zhang Q X, Zhou Y H. Strengthening of cold-setting resin sand by the additive method. *Journal of Materials Processing Technology*, 1997, 72(2): 239–242.
- [2] Robert A L, Michael M G. The development of hardened furan resin. *Modern Casting*, 1997, 87(10): 33–35.
- [3] John R. Brown. *Foseco Ferrous Foundryman's Handbook* (Eleventh Edition). London: Butterworth Heinemann Publisher, 2000: 167–203.
- [4] Fox J T, Cannon F S, Brown N R, et al. Comparison of a new, green foundry binder with conventional foundry binders. *International Journal of Adhesion and Adhesives*, 2012, 34: 38–45.
- [5] Siddique R, Schutter G, Noumowe A. Effect of used-foundry sand on the mechanical properties of concrete. *Construction and Building Materials*, 2009, 23 (2): 976–980.
- [6] Wen Z G, Li H F. Analysis of potential energy conservation and CO₂ emissions reduction in China's non-ferrous metals industry from a technology perspective. *International Journal of Greenhouse Gas Control*, 2014, 28: 45–56.
- [7] Huisingh D, Zhang Z H, Mooreb J C, et al. Recent advances in carbon emissions reduction: policies, technologies, monitoring, assessment and modeling. *Journal of Cleaner Production*, 2015, 103 (15): 1–12.
- [8] Lazzarin R M, Noro M. Energy efficiency opportunities in the production process of cast iron foundries: An experience in Italy. *Applied Thermal Engineering*, 2015, 90(5): 509–520.
- [9] Thollander P, Backlund S, Trianni A, et al. Beyond barriers—A case study on driving forces for improved energy efficiency in the foundry industries in Finland, France, Germany, Italy, Poland, Spain, and Sweden. *Applied Energy*, 2013, 111: 636–643.
- [10] Zanetti M C, Fiore S. Foundry processes: The recovery of green moulding sands for core operations. *Resources, Conservation and Recycling*, 2003, 38(3): 243–254.
- [11] Cruz N, Briens C, Berruti F. Green sand reclamation using a fluidized bed with an attrition nozzle. *Resources, Conservation and Recycling*, 2009, 54(1): 45–52.
- [12] Sun Q Z, Xu R F, Zhao Z K, et al. Reclamation of green sand containing hot-box resin sand and its application. *Advanced Materials Research*, 2010, 97–101: 1037–1040.
- [13] Fiore S, Zanetti M C. Industrial treatment processes for recycling of green foundry sands. *International Journal of Cast Metals Research*, 2008, 21(6): 435–438.
- [14] Kurokawa Y, Kambayashi H, Ota H, et al. Reclamation Mechanism of Waste Green Sand Adhered with Oolitics. *Journal of Japan Foundry Engineering Society*, 1999, 71(7): 468–474.
- [15] Zanetti M C, Fiore S. Foundry processes: The recovery of green moulding sands for core operations. *Resources, Conservation and Recycling*, 2003, 38(3): 243–254.
- [16] Manabe T, Yamamoto Y, Hoshiyama Y. Effect of using furan resin reclamation sand in evaporative pattern casting process. *Transactions of the American Foundry Society*, 2005, 113: 1029–1037.

- [17] Kamińska J, Dańko J. Preliminary research on granulation process of dust waste from reclamation process of moulding sands with furan resin. *Archives of Foundry Engineering*, 2012, 12(3): 53–58.
- [18] Holtzer M, Drożyński D, Bobrowski A, et al. The influence of reclaim on properties of moulding sand with furan resin. *Archives of Foundry Engineering* 2010, 10(2): 61–64.
- [19] Guigo N, Mija A, Vincent L, et al. Eco-friendly composite resins based on renewable biomass resources: polyfurfuryl alcohol/lignin thermosets. *European Polymer Journal*, 2010, 46(5): 1016–1023.
- [20] Fan Z T, Huang N Y, Wang H F, et al. Dry reusing and wet reclaiming of used sodium silicate sand. *China Foundry*, 2002, 2(1): 38–43.
- [21] Fan Z T, Huang N Y, Dong X P. In house reuse and reclamation of used foundry sands with sodium silicate binder. *International Journal of Cast Metals Research*, 2004, 17(1): 51–56.
- [22] Stachowicz M, Granat K. Influence of melt temperature on strength parameters of cyclically activated used-up sandmixes containing water-glass, hardened with microwaves. *Archives of Civil and Mechanical Engineering*, 2015, 15(4): 831–835.
- [23] GB/T 2684. Test methods for foundry sands and molding mixtures. State Standard of the People's Republic of China, 2009. (In Chinese)
- [24] Abbas H H, Salih R A. Synthesis, characterization, thermal degradation and electrical conductivity of salicylidene-anthranilic acid-schiff base formaldehyde resin (R-AASA). *Chinese Journal of Polymer Science*, 2009, 27(4): 465–477.
- [25] Guigo N, Mija A, Zavaglia R, et al. New insights on the thermal degradation pathways of neat poly (furfuryl alcohol) and poly (furfuryl alcohol)/SiO₂ hybrid materials. *Polymer Degradation and Stability*, 2009, 94 (6): 908–913.
- [26] Monti M, Hoydonckx H, Stappers F, et al. Thermal and combustion behavior of furan resin/silica nanocomposites. *European Polymer Journal*, 2015, 67: 561–569.
- [27] Dungan R S, Reeves III J B. Pyrolysis of foundry sand resins: a determination of organic products by mass spectrometry. *Journal of Environmental Science and Health, Part A*, 2005, 40 (8):1557–1567.
- [28] Ren Y Y, Li Y M. Substitute materials of furfuryl alcohol in furan resin used for foundry and their technical properties. *China Foundry*, 2009, 4: 339–342.
- [29] KAYAL S, Chakrabarti B K. Reclamation and utilization of foundry waste sand. *High Temperature Material and Sciences*, 2008, 27: 51–60.
- [30] Wang J N, Fan Z T, Zan X L, et al. Properties of sodium silicate bonded sand hardened by microwave heating. *China Foundry*, 2009, 6 (3): 191–196.
- [31] Loto C A, Adebayo H. Effects of variation in water content, clay fraction and sodium carbonate additions on the synthetic moulding properties of igbokoda clay and silica sand. *Applied Clay Science*, 1990, 5 (2):165–181.
- [32] Olasupo O A, Omotoyinbo J A. Moulding properties of a Nigerian silica-clay mixture for foundry use. *Applied Clay Science*, 2009, 45(4): 244–247.
- [33] Stachowicz M, Granat K, Nowak D. Application of microwaves for innovative hardening of environment-friendly water-glass moulding sands used in manufacture of steel castings. *Archives of Civil and Mechanical Engineering*, 2011, 11(1): 209–219.

This project is sponsored by the National Natural Science Foundation of China (Nos. 51275295 and 51201102), the Shanghai Rising-Star Program (No. 14QB1403200), Research Fund for the Doctoral Program of Higher Education of China (Nos. 20120073120011 and 20130073110052).
